

Soliton-induced dislocations and discrete solitons in partially-coherent photonic lattices

Hector Martin¹, Eugenia D. Eugenieva² and Zhigang Chen^{1,3}

¹ *Department of Physics and Astronomy, San Francisco State University, CA 94132*

² *Intel Corporation, USA,* ³ *TEDA College, Nankai University, China*

zchen@stars.sfsu.edu

Demetrios N. Christodoulides

School of Optics/CREOL, University of Central Florida, Orlando, FL 32816

Abstract: We investigate the interaction between a light beam and a two-dimensional photonic lattice that is photo-induced in a photorefractive crystal using partially coherent light. We demonstrate that this interaction process is associated with a host of new phenomena including lattice dislocation, lattice deformation, and creation of structures akin to optical polarons. In addition, two-dimensional discrete solitons are realized in such partially coherent photonic lattices.

PACS numbers: 42.65.-k, 42.65.Tg, 05.45Yv

Closely-spaced nonlinear waveguide arrays have recently been the focus of considerable attention. This is due, in part, to their strong link with the emerging science and technology of nonlinear photonic crystals and their ability to discretize light propagation [1, 2]. In such array structures, the collective behavior of wave propagation exhibits intriguing phenomena that are also encountered in many other discrete nonlinear systems, for example in biology, solid state physics and Bose-Einstein condensates [3-5]. In optics, the diffraction dynamics of a light beam is profoundly affected even in linear waveguide lattices due to evanescent coupling between nearby waveguide sites, leading to discrete diffraction [6, 7]. If the waveguide array is embedded in a nonlinear medium, more interesting wave behavior is expected to occur. For instance, a balance between discrete diffraction and nonlinear self-focusing can lead to optical self-trapped states better known as discrete solitons (DCS) [1, 6]. In nonlinear optics, DCS were predicted in 1988 [1], and were demonstrated in one-dimensional (1D) AlGaAs semiconductor waveguide arrays ten years later [6]. Recently, a theoretical study suggested that DCS could also form in optically-induced waveguide arrays [8]. This soon led to the experimental observation of two-dimensional (2D) DCS in such waveguide arrays induced via coherent beam interference [9]. Meanwhile, partially coherent pixel-like beams have also been successfully employed to establish stable 2D photonic lattices in the bulk of a photosensitive crystal [10]. In this latter configuration, the lattice itself experiences a strong nonlinearity, and as a result, it becomes considerably more susceptible to soliton-induced deformation. This in turn brings about the interesting possibility of studying optical soliton-lattice interactions that might exhibit many of the basic characteristic features of other physical processes such as those encountered in polaron excitation/formation in solid state physics [11].

In this Letter, we report the first experimental observation of soliton-induced dislocation/deformation and DCS in photonic lattices created by partially coherent light. By exploiting the anisotropic properties of the photorefractive nonlinearity, the waveguide lattices can be conveniently operated in either the linear or nonlinear regime [8]. In the nonlinear regime, by launching a soliton (probe) beam into such a lattice, we observe transverse velocity slow-down of the probe as well as soliton-induced lattice dislocation, and creation of optical structures that are analogous to polarons in solid state physics. Conversely, when the lattice is operated in the linear regime, so that itself does not

experience any strong nonlinearity during propagation, we observe that the probe beam evolves from discrete diffraction to DCS as the level of nonlinearity for the probe is increased. We emphasize that, different from previous experiment [9], the DCS reported in this study are hosted in partially incoherent photonic lattices. This in turn enables, through coherence control, stable lattice formation due to suppression of modulation instabilities [12, 13]. Our experimental results are in good agreement with the theoretical analysis of these effects.

The experimental setup for our study is similar to those used in Refs [10, 14]. A partially spatially incoherent beam ($\lambda=488$ nm) is created with a rotating diffuser, and a biased photorefractive crystal (SBN:60, $5 \times 5 \times 8$ mm³, $r_{33}=280$ pm/V and $r_{13}=24$ pm/V) is employed to provide a self-focusing noninstantaneous nonlinearity, as in previous demonstration of incoherent solitons [15]. To generate a 2D-waveguide lattice, we use an amplitude mask to spatially modulate the otherwise uniform incoherent beam after the diffuser. The mask is then imaged onto the input face of the crystal, thus creating a pixel-like input intensity pattern [10]. A Gaussian beam split from the same laser is used as the probe beam propagating along with the lattice. In addition, a uniform incoherent background beam is used as "dark illumination" for fine-tuning the nonlinearity [16].

In our experiment, the probe beam is extraordinarily polarized and "*fully*" *coherent* (i.e., it does not pass through the diffuser), while the lattice beam is *partially coherent* and its polarization can be either extraordinary (*e*) or ordinary (*o*) as needed. In general, in an anisotropic photorefractive crystal, the nonlinear index change experienced by an optical beam depends on its polarization as well as its intensity. Under appreciable bias conditions, i.e., when the photorefractive screening nonlinearity is dominant [16], this index change is approximately given by $\Delta n_e = [n_e^3 r_{33} E_0 / 2](1 + I)^{-1}$ and $\Delta n_o = [n_o^3 r_{13} E_0 / 2](1 + I)^{-1}$ for e-polarized and o-polarized beams, respectively. Here E_0 is the applied electric field along the crystalline c-axis (x-direction), and I is the intensity of the beam normalized to the background illumination. Due to the difference between the nonlinear electro-optic coefficient r_{33} and r_{13} , Δn_e is more than 10 times larger than Δn_o (in the SBN crystal we used) under the same experimental conditions. Thus, when it is extraordinarily polarized, the lattice beam experiences a nonlinear index change comparable to the probe beam, whereas it evolves almost linearly when it is ordinarily polarized. As mentioned before, since our lattice beam is partially coherent and has

been created by amplitude modulation rather than by coherent multi-beam interference [9], our waveguide lattice remains stable even in the nonlinear regime due to suppression of modulation instabilities [12, 13]

First, we present experimental results on the interaction of a probe beam with a waveguide lattice induced by 2D pixel-like spatial solitons. In this case, both the probe and the lattice beam are extraordinarily polarized. Under appropriate conditions, a stable soliton array is first established and then, the probe beam is launched into one of the induced waveguides. If the intensity of the probe is much weaker than that of the lattice, the probe beam is simply guided by the waveguide channel, and it does not affect the lattice. However, once the intensity of the probe beam becomes comparable to that of the lattice, the probe beam forms a soliton itself and thus plays a role in the interaction process, which in turn leads to interesting dynamics between the probe/soliton and the partially coherent lattice. Typically, when the probe beam is launched at one of the waveguides at a small angle relative to the propagation direction of the lattice, we observe lattice dislocation due to soliton dragging. Figure 1 shows an example of such an interaction. For this experiment, the coherence length of the partially coherent lattice is $40\text{ }\mu\text{m}$, and its intensity is about 3 times higher than that of the background beam. The lattice spacing is $70\text{ }\mu\text{m}$, and the intensity FWHM of each soliton is $17\text{ }\mu\text{m}$. This 2D lattice was created at a bias field of 2400 V/cm . When the probe beam with an intensity equal to that of the lattice was launched into one of the lattice sites at a shallow angle ($\sim 0.5^\circ$) either to the right [Fig. 1(a)] or to the left [Fig. 1(b)], the lattice overall remained uniform except for a dislocation created by the probe beam. Meanwhile, the probe beam itself retained its soliton identity, but its lateral shift (at the crystal output) was reduced significantly because of interaction with the lattice, indicating a slow-down in its transverse velocity [Fig. 1(c) and 1(d)]. Without the lattice, the probe beam traveled $68\text{ }\mu\text{m}$ in the x-direction (the spot far away from the center), whilst under the same conditions, it traveled only about $26\text{ }\mu\text{m}$ when interacting with the lattice (the spot close to the center). These two photographs were taken separately and then superimposed in the same figure. A slight difference was observed between launching the probe beam towards and against the crystalline c-axis because of diffusion-induced effect [16].

Our experimental observations are corroborated by numerical simulations. The evolution of the partially coherent lattice is described by the so-called coherent density approach [17], whereas that of the coherent probe beam by a paraxial nonlinear wave equation:

$$i\left(\frac{\partial f}{\partial z} + \mathbf{q}_x \frac{\partial f}{\partial x} + \mathbf{q}_y \frac{\partial f}{\partial y}\right) + \frac{1}{2k}\left(\frac{\partial^2 f}{\partial x^2} + \frac{\partial^2 f}{\partial y^2}\right) - \mathbf{b} \frac{1}{1+I_N} f = 0, \quad (1)$$

$$i\frac{\partial u}{\partial z} + \frac{1}{2k}\left(\frac{\partial^2 u}{\partial x^2} + \frac{\partial^2 u}{\partial y^2}\right) - \mathbf{b} \frac{1}{1+I_N} u = 0, \quad (2)$$

$$I_N(x, y, z) = \int_{-\infty}^{\infty} \int_{-\infty}^{\infty} \left| f(x, y, z, \mathbf{q}_x, \mathbf{q}_y) \right|^2 d\mathbf{q}_x d\mathbf{q}_y + I_C(x, y, z), \quad (3)$$

where the coherent density function f at the input is expressed as $f(x, y, \mathbf{q}_x, \mathbf{q}_y, z=0) = r^{1/2} G_N^{1/2}(\mathbf{q}_x, \mathbf{q}_y) \Phi_0(x, y)$, and $I_C = |u|^2$ is the intensity of the probe beam co-propagating with the lattice. In Eqs. (1-3), $I_N = I / I_b$ is the normalized total intensity with respect to the background illumination, and the integral term in Eq. (3) represents the intensity of the partially coherent lattice. The intensity ratio r is defined as $r = I_{\max} / I_b$, with I_{\max} being the initial maximum intensity of the lattice. \mathbf{q}_x and \mathbf{q}_y are the angles at which the coherent density propagates with respect to the z axis. The nonlinear constant, $\mathbf{b} = k_0 E_0 n^3 r_{\text{eff}} / 2$, is determined by the crystal parameters and the bias field E_0 , where $k_0 = 2\pi / \lambda$ is the wave number, n is the refractive index of the crystal, and the effective electrooptic coefficient for SBN:60 is $r_{\text{eff}} = (r_{33}, r_{13})$ depending on the polarization. The function G_N represents the initial distribution of the angular power spectrum of the incoherent beam and is here taken to be Gaussian: $G_N(\mathbf{q}_x, \mathbf{q}_y) = (\mathbf{p} \mathbf{q}_0^2)^{-1} \exp[-(\mathbf{q}_x^2 + \mathbf{q}_y^2) / \mathbf{q}_0^2]$, and the associated spatial coherence length is given by $l_c = \lambda / \sqrt{2\pi n \mathbf{q}_0}$. $\Phi_0(x, y)$ is the spatial modulation function for the incoherent beam as imposed by the amplitude mask. Eqs. (1-3) were solved numerically using a fast Fourier transform multi-beam propagation method. Figure 2 shows simulations of a typical soliton-lattice interaction in a 7x7 induced waveguide lattice established by a partially coherent beam, where both the probe and the lattice beam are extra-ordinarily polarized. Soliton-induced lattice dislocations as well as slow-down in the transverse velocity of the probe beam are evident in simulations in agreement with the observed experimental behavior. Figure 2(a) depicts the output intensity pattern of the lattice when the probe beam is launched at an angle of 0.5° towards +x-direction, and Fig. 2(b) shows the output intensity profile of the probe beam in the presence (solid line) or absence (dashed line) of the lattice

under the same conditions. A 15% slow-down in the transverse velocity of the probe is observed after 8-mm of propagation. Similar numerical results were obtained when the probe is launched at the same angle towards $-x$ -direction.

When the lattice spacing was decreased by use of different masks, other interesting phenomena were observed. These include generation of defects, strong lattice deformation, and polaron-like structures in the lattice. Typical results are illustrated in Fig. 3, for which the spacing of the lattice is about $55\text{ }\mu\text{m}$ and its coherence length is $40\text{ }\mu\text{m}$. At this lattice spacing, when the probe beam was launched straight into one of the waveguide channels, a polaron-like induced structure was observed, in which the probe soliton dragged towards it some of the neighboring sites while pushing away the other [Fig. 3(a)]. For comparison, Fig. 3(b) shows the corresponding restored lattices after the probe beam was removed and the crystal reached a new steady-state under the same conditions. When the probe beam intensity was much higher than that of the lattice, the lattice structure became strongly deformed in such a way that the site dislocations extended beyond the immediate neighborhood [Fig. 3(c)]. The polaron-like structure was reproduced with different lattice spacing, and the effect became more pronounced when the lattice spacing was reduced to about $40\text{ }\mu\text{m}$. The observed process is quite similar to that caused by a polaron in solid state physics during which an electron drags and dislocates heavy ions as it propagates through an ionic crystal [11]. Since our lattice itself is partially coherent and its spacing is larger than the coherence length, nearby pixels in the lattice have no (or only weak) initial phase correlation. In addition, the lattice is mutually incoherent with the probe. Thus, one would expect only attraction between nearby lattice sites rather than repulsion [18]. The observed polaron-like interaction instead suggests that the probe beam has induced certain degree of coherence to the nearby lattice sites with different phase correlation.

When the lattice spacing was further decreased below $40\text{ }\mu\text{m}$, the formation of the soliton lattice required a much higher nonlinearity, which caused the lattice to be unstable due to strong modulation instability. To create a stable lattice with a smaller spacing, we switched the polarization of the lattice beam from extra-ordinary to ordinary. As discussed earlier, the lattice in this configuration (o-polarized) “sees” only a weak nonlinearity as compared to that experienced by the e-polarized probe beam, and therefore remains nearly invariant as the bias field increases. At the same time, the partially coherent lattice provides linear waveguiding for the probe beam. Typical experimental results are presented in Fig.

4, in which a lattice with a small spacing of $20\text{ }\mu\text{m}$ was first generated. A probe beam (with intensity 4 times weaker than that of the lattice) was then launched into one of the waveguide channels, propagating collinearly with the lattice. Due to weak coupling between closely spaced waveguides, the probe beam underwent discrete diffraction when the nonlinearity was low, whereas it formed a 2D discrete soliton at an appropriate level of high nonlinearity. The lattice itself was not considerably affected by the weak probe or the increased bias field. The first two photographs show the Gaussian-like probe beam at the crystal input [Fig. 4(a)] and its linear diffraction at the crystal output after 8 mm of propagation [Fig. 4(b)]. Discrete diffraction in the square lattice was observed at a bias field of 900 V/cm [Fig. 4 (c)], clearly showing that most of the energy flows from the center towards the diagonal directions of the lattice. Even more importantly, at a bias field of 3000 V/cm , a DCS was observed [Fig. 4(d)], with most of energy concentrated in the center and the four neighboring sites along the principal axes of the lattice. (Animations of the process can be viewed online [19]). These experimental results are truly in agreement with expected behavior from the theory of discrete systems [8, 20]. We emphasize that, for such a DCS, a delicate balance has been reached between waveguide coupling offered by the lattice and the self-focusing experienced by the probe beam through fine-tuning the experimental parameters. Different from previous experiment [9], the DCS reported here are hosted in partially incoherent photonic lattices, where the spatial coherence provides an additional degree of freedom in controlling the above processes.

In summary, we have demonstrated novel interaction between a light beam and a 2D photonic lattice induced by partially coherent light that leads to a host of new phenomena including lattice dislocation, lattice deformation, and creation of structures akin to optical polarons. Furthermore, 2D discrete solitons have been successfully demonstrated in partially-coherent lattices. Our results may pave the way to observe similar phenomena in other relevant discrete nonlinear systems.

This work was supported by AFOSR, Research Corp., ARO MURI, and a grant from the Pittsburgh Supercomputing Center. We thank L. Zimmerman, M. Segev and J. Xu for assistance.

References:

- [1] D. N. Christodoulides and R. I. Joseph, *Opt. Lett.* **13**, 794 (1988).
- [2] S. Mingaleev and Y. Kivshar, *Opt. & Photonics News*, Vol. **13**, 48 (2002).
- [3] A. S. Davydov, *Biology and Quantum Mechanics* (Pergamon, Oxford, 1982).
- [4] A. J. Sievers and S. Takeno, *Phys. Rev. Lett.* **61**, 970 (1988).
- [5] A. Trombettoni and A. Smerzi, *Phys. Rev. Lett.* **86**, 2353 (2001).
- [6] H. S. Eisenberg et al., *Phys. Rev. Lett.* **81**, 3383 (1998);
R. Morandotti et al., *Phys. Rev. Lett.* **83**, 2726 (1999).
- [7] F. Lederer and Y. Silberberg, *Opt. & Photonics News*, Vol. **13**, 48 (2002).
- [8] N. K. Efremidis et al., *Phys. Rev. E* **66**, 046602 (2002).
- [9] J. W. Fleischer, et al., *Nature* **422**, 150 (2003).
- [10] Z. Chen and K. MaCarthy, *Opt. Lett.* **27**, 2019 (2002).
- [11] C. Kittel, *Introduction to Solid State Physics* (John Wiley & Sons, New York, 1996).
- [12] M. Soljacic et al., *Phys. Rev. Lett.* **84**, 467 (2000).
- [13] D. Kip et al., *Science* **290**, 495 (2000).
- [14] Z. Chen et al., *Phys. Rev. E* **66**, 066601 (2002).
- [15] M. Mitchell et al., *Phys. Rev. Lett.* **77**, 490 (1996); Z. Chen et al., *Science* **280**, 889 (1998).
- [16] M. Segev et al., *Phys. Rev. Lett.* **73**, 3211 (1994).
- [17] D. N. Christodoulides et al., *Phys. Rev. Lett.* **78**, 646 (1997).
- [18] G. I. Stegeman, M. Segev, *Science* **286**, 1518 (1999).
- [19] Animations of DCS formation as obtained from experiment can be viewed at
www.physics.sfsu.edu/~laser/.
- [20] J. Hudock et al., "Elliptical discrete solitons in waveguide arrays", *Opt. Lett.*, submitted.

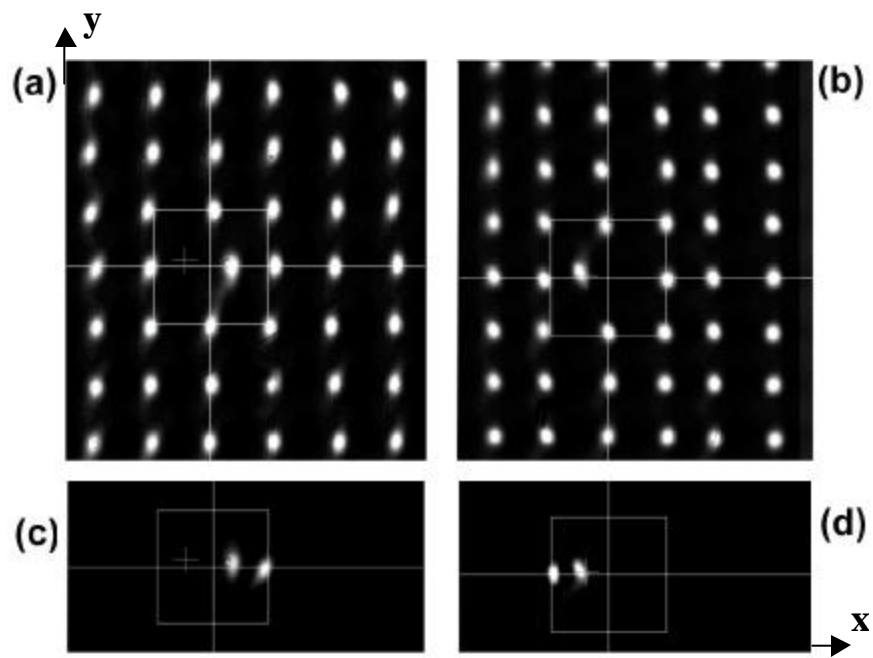
Figure Captions:

Fig. 1: Soliton-induced lattice dislocation when a probe beam was launched towards (a) the right and (b) the left at 0.5° . (c) and (d) show a slow-down in the transverse velocity of the probe beam.

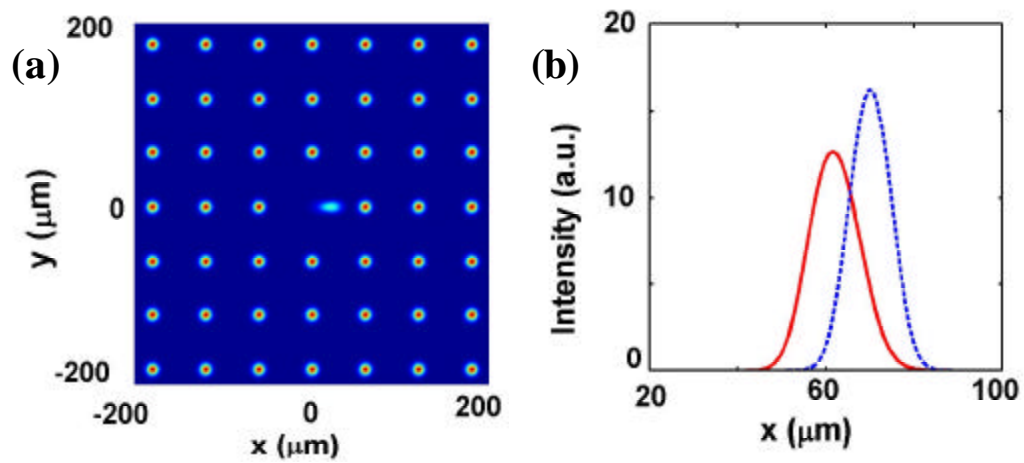
Fig. 2: Numerical results corresponding to Fig. 1(a) and Fig. 1(c).

Fig. 3: Soliton-induced polaron-like structure (a) and a strongly deformed lattice (c). (b) shows the restored lattice of (a) after the probe beam is turned off.

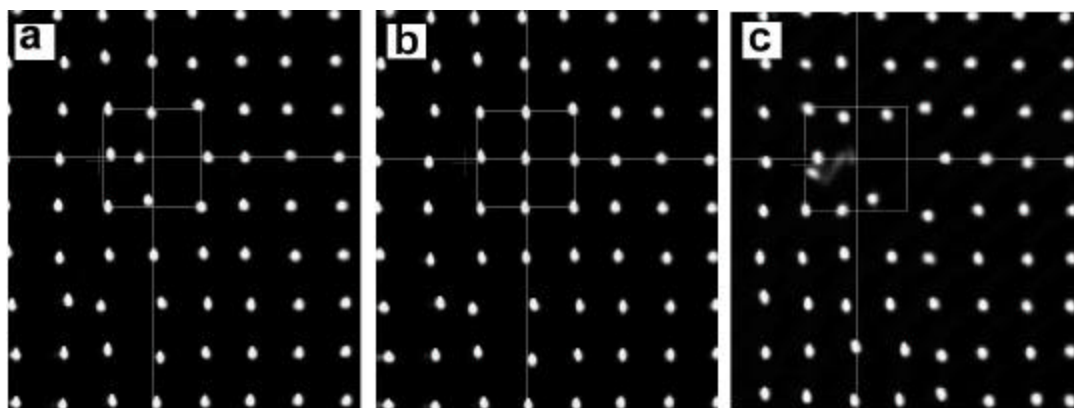
Fig. 4: Demonstration of a 2D discrete soliton in a partially coherent lattice. (a) input, (b) diffraction output without the lattice, (c) discrete diffraction at 900 V/cm, and (d) discrete soliton at 3000 V/cm.



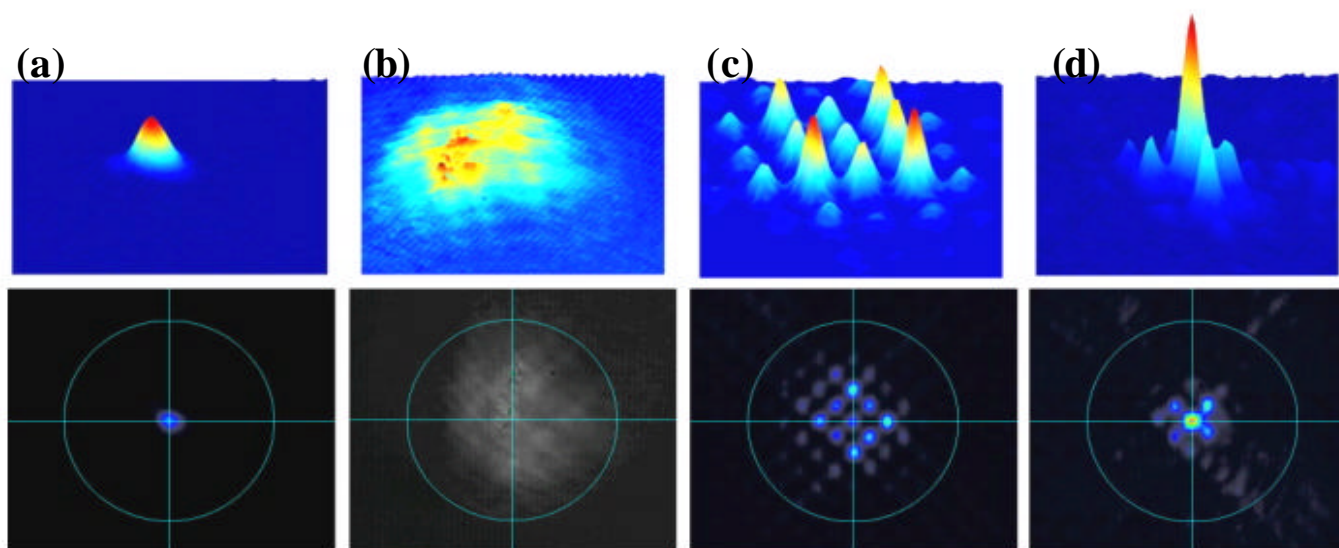
Martin et al. Fig 1



Martin et al., Fig. 2



Martin et al., Fig. 3



Martin et al., Fig. 4